About the performance of nonlinear tuned mass damper on the nonlinear dynamic controlled equation

Zenón J. G. N. del Prado[1], Marcello G. Marques Filho[1]

[1]*School of Civil and Environmental Engineering, Federal University of Goiás*
Avenida Universitária, 74605-220, Goiânia/GO, Brazil
zenon@ufg.br, marcellogomes@discente.ufg.br

Abstract. In this work, the performance of a nonlinear tuned mass damper is evaluated when applied to a nonlinear Duffing equation with both softening and hardening behavior. For this, a damped Duffing nonlinear oscillator is considered and subjected to a harmonic load, first the optimal linear control parameters are obtained and these parameters are used to evaluate its performance on the nonlinear vibration regime. The quality of the nonlinear tuned mass damper is observed on the resonance curves, basin of attraction, time responses, phase planes and Poincaré sections.

Keywords: tuned mass damper, Duffing equation, nonlinear tuned.

1 Introduction

The tuned mass damper (TMD) is a device proposed by Frahm [1] to suppress the steady-state response of an undamped mass-spring system, subjected to a harmonic load, which is effective when the harmonic load frequency was constant. Ormondroyd and Den Hartog [2] proposed the introduction of the damping on the TMD, in order to improve its performance when the frequency varies.

Den Hartog [3] observed that the resonance curves of the system always pass through two invariant points. So, it was proposed that the TMD stiffness was adjusted so the two points has the same height and the absorber damping was adjusted so the curve has a horizontal tangent through one of the fixed points. This method is usually called the Den Hartog's Equal Peak Method.

It was observed by Habib *et al*. [4] that the resonances of a non-linear mechanic system were better reduced by a non-linear tuned vibration absorber (NLTVA), which has a non-linearity of the same mathematical form of the main structure and was developed to ensure equal peaks in the resonance curves for a larger range of forcing amplitudes. Later, Habib and Kerschen [5] developed a similarity principle for a NLTVA attached to a nonlinear structure, deriving an analytical equation to obtain the nonlinear coefficient of the absorber, which is valid for any polynomial nonlinearity in the primary system and depends only on the mass ratio and the nonlinear coefficient of the primary system. When the primary system has several polynomial nonlinearities, it was observed that each nonlinear coefficient can be calculated independently of the other nonlinear coefficients.

Detroux *et al*. [6] presented a performance, robustness and sensitivity analysis of the NLTVA attached to a Duffing oscillator. The parameter space of the NLTVA was studied, identifying boundaries that delimit safe, unsafe and unacceptable operations, using a combination of numerical continuation of periodic solutions, global analysis and bifurcation detecting and tracking.

The Duffing oscillator is a well-studied system in non-linear dynamics, being initially studied by Georg Duffing. This system can be used to model various physical process as spring stiffnesses, buckling of beams, non-linear electronic circuits and ionization waves in plasmas [7].

The main purpose of this work is to analyze the performance of nonlinear systems composed by a damped Duffing oscillator with a nonlinear tuned vibration absorber (NLTVA) attached. The nonlinearity of the system is studied by the means of a cubic stiffness spring, considering the possibilities of hardening and softening behavior

for both the oscillator and the absorber.

2 Mathematical formulation

Consider a main dynamical system with mass m_1, damping c_1, linear stiffness k_1, non-linear cubic stiffness k_{nl1} and subjected to a harmonic external load $F(t) = F\cos(\Omega t)$ as observed in Fig. 1(a). To perform vibration control, a non-linear control device is attached to the main system with mass m_2, damping c_2, linear stiffness k_2 and nonlinear cubic stiffness k_{nl2}. Figure 1(b) depicts the free body diagram of the system, from which, applying the 2nd Newton Law, the dynamic equations of motion are obtained, as presented in Eq. (1).

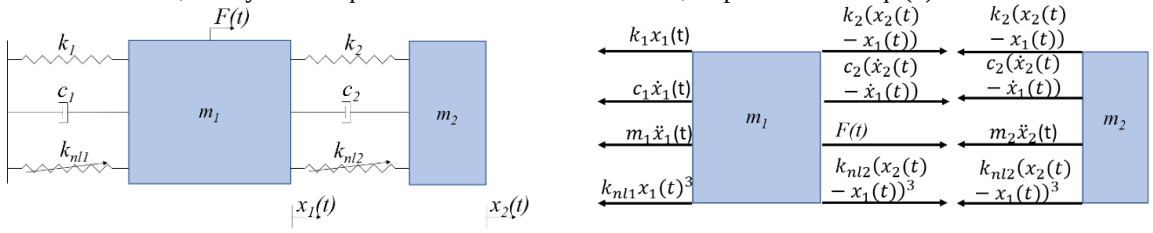

(a) (b)

Figure 1. (a) Mechanical model of the system. (b) Free body diagram.

$$\begin{aligned} m_1\ddot{x}_1 + k_1x_1 + k_{nl1}{x_1}^3 + c_2(\dot{x}_1 - \dot{x}_2) + k_2(x_1 - x_2) + k_{nl2}(x_1 - x_2)^3 = F\cos(\Omega t). \\ m_2\ddot{x}_2 + c_2(\dot{x}_2 - \dot{x}_1) + k_2(x_2 - x_1) + k_{nl2}(x_2 - x_1)^3 = 0. \end{aligned} \quad (1)$$

To study the influence of the NLTVA on the dynamic response of the main system, four different cases of nonlinearity were considered as: a) Case 1: Main (hardening) and NLTVA (hardening); b) Case 2: Main (softening) and NLTVA (hardening); c) Case 3: Main (softening) and NLTVA (softening) and d) Case 4: Main (hardening) and NLTVA (softening).

For each case studied, a linear optimization of the system is performed, based on Den Hartog's Equal Peak Method [3]. Case 1 uses parameter values presented by Detroux *et al.* [6], so the results obtained can be compared to previous published results, to assure the methodology adopted is performing well. For Cases 1 and 4, where the main structure has hardening behavior and very small damping, the linear optimization used the equations proposed by Asami and Nishihara [8], because they provide an exact solution for undamped main structures.

In Cases 2 and 3, where the main structure has softening behavior and higher damping, the parameters were chosen by the authors of this paper and the equations proposed by Tsai and Lin cited by Connor and Laflamme [9] are applied, so the optimal linear stiffness and damping coefficient of the NLTVA are obtained, considering the higher damping coefficient adopted to the main structure. The results of the linear optimization and the cases studied are presented in Tab. 1.

Table 1. Cases studied and parameters of the Duffing oscillator and attached NLTVA.

Case	*Main Structure*	*NLTVA*	m_1 *(kg)*	k_1 *(N/m)*	c_1 *(Ns/m)*	knl_1 *(N/m³)*	m_2 *(kg)*	k_2 *(N/m)*	c_2 *(Ns/m)*
Case 1	Hardening	Hardening	1	1	0.002	1	0.05	0.0454	0.0128
Case 2	Softening	Hardening	1	1	0.1	-0.05	0.05	0.0417	0.0131
Case 3	Softening	Softening	1	1	0.1	-0.05	0.05	0.0417	0.0131
Case 4	Hardening	Softening	1	1	0.002	1	0.05	0.0454	0.0128

The nonlinear optimization is performed so the optimal cubic stiffness for each Case is obtained, by evaluating the amplitude of the peaks in the frequency-response of the system for several values of cubic stiffness. The frequency-response of the system were obtained with the algorithm proposed by del Prado [10], based on brute force integrations.

After that, the 4th order Runge-Kutta Method is used to obtain the time-response, phase planes and Poincaré sections for the optimized systems. Then, the algorithm proposed by del Prado [10] is used to obtain the basins of attraction, so the effect of the initial conditions over the overall performance of the systems is analyzed.

3 Numerical results

First, the nonlinear optimization is performed for Case 1, in which both the main structure and the NLTVA display *hardening* behavior, by fixing the amplitude of harmonic force $F = 0.05$, varying the cubic stiffness of the absorber knl_2 and getting the resonance curves with del Prado's brute force method [10] to observe the resonance peaks as presented in Fig. 2. For knl_2 equal to 0.0, 1.0e-4 and 1.0e-3, the second resonance peak has higher amplitudes, meanwhile for knl_2 equal to 1.0e-2, the first resonance peak has higher amplitudes. The optimal parameter was obtained for knl_2 equal to 4.0e-3, which is very close from the value 4.2e-3 obtained by Detroux *et al.* [6].

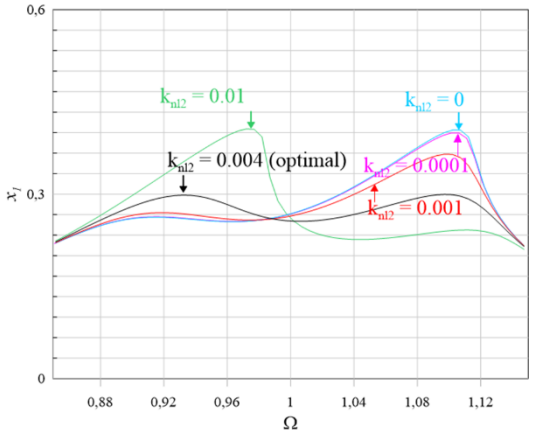

Figure 2. Nonlinear optimization for Case 1.

Figure 3 displays the comparison of resonance curve and basin of attraction for $F = 0.15$ N and $\Omega = 2.0$ with previous results obtained by Detroux *et al.* [6]. Figure 3(a) shows the resonance curve where black color represents stable solutions and red color represents unstable solutions and were obtained using both force brute method and continuation techniques. As can be observed, as the value of load frequency is incremented, the amplitude *a* increases until certain value where it shows unstable solutions and a window with co-existence of stable and quasi-periodic oscillations and, if the load frequency is increased, the system displays small stable 1T oscillations. The basis of attraction of Fig. 3(b) shows two attractors, yellow color is related to the small amplitude attractors and blue color to large amplitude attractor. As can be seen, obtained resonance curve and basin of attraction are very similar with results from Detroux *et al.* [6], except for a detached resonance curve (DRC) with higher amplitudes.

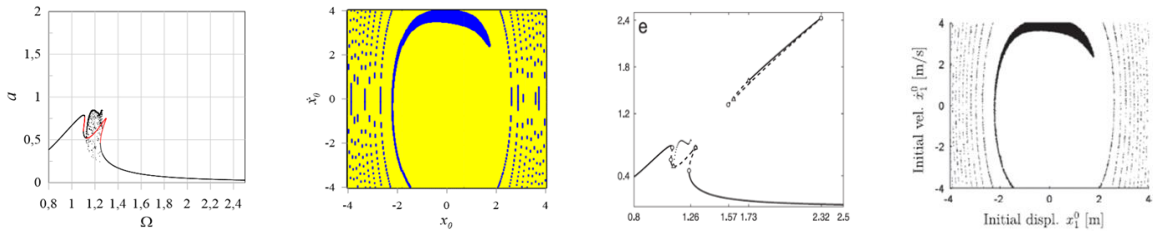

(a) (b) (c) (d)

Figure 3. Resonance curve and basin of attraction for Case 1. (a) Obtained resonance curve, (b) Obtained basin of attraction, (c) Resonance curve from Detroux *et al.* [6] and d) Basin of attraction from Detroux *et al.* [6].

Figure 4 depicts the time-responses, phase spaces and Poincaré maps of points with initial conditions in the resonance curves and basin of attraction. Figure 4(a) and (b) shows the time response and Poincaré 1T map of a point corresponding to small amplitude attractor of the basin of attraction (yellow color), Fig. 4(c) and (d) shows the time response and Poincaré 1T map of a point corresponding to large amplitude attractor of the basin of attraction (blue color) and Fig. 4(e) and (f) shows the time response and Poincaré corresponding to the window of

quasi-periodic oscillations in Fig. 3(a). The small amplitude attractor leads to displacements in the order of 0.07 m meanwhile the large amplitude attractor leads to displacements in the order of 1.8 m, which is related to the DRC presented by Detroux *et al.* [6]. By adopting F = 0.11 and Ω = 0.14955, the system responds in a quasi-periodic regime of motion, as can be seen in Fig. 3 (e), (f).

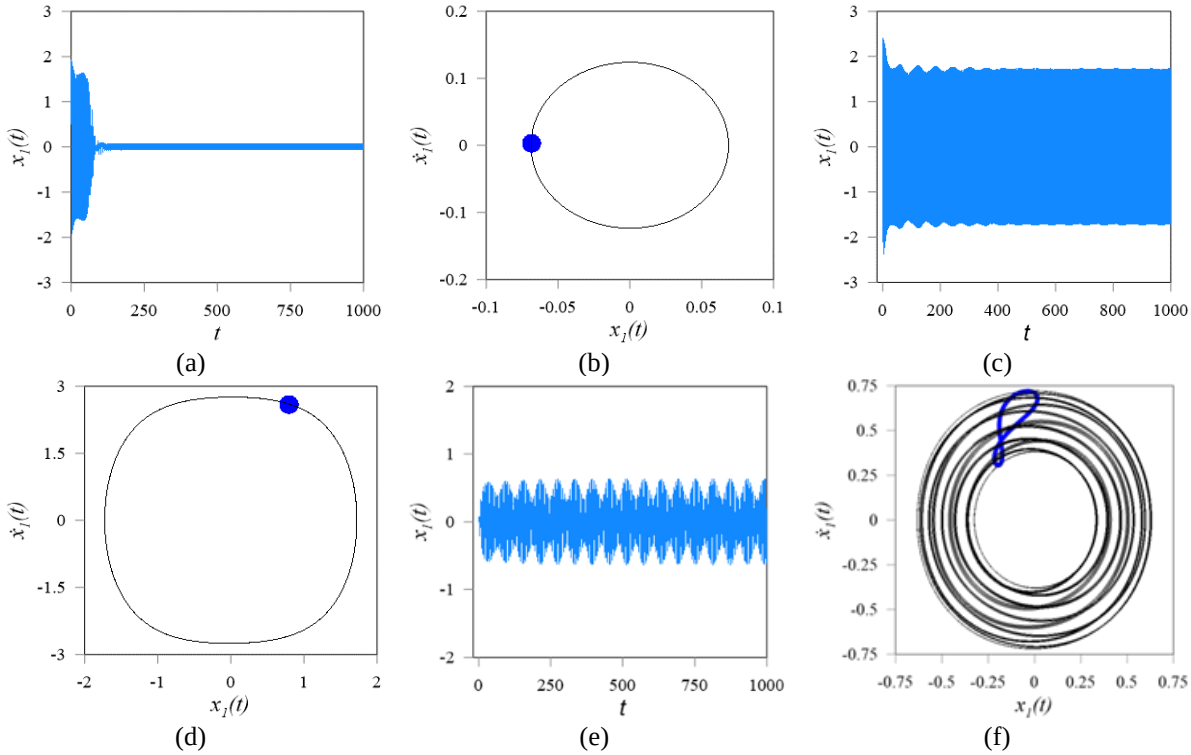

Figure 4. Time-response, phase plane and Poincaré sections for Case 1. (a) Time response for small amplitude, (b) Small amplitude phase plane, (c) Time response for large amplitude. (d) Large amplitude phase plane, (e) Time response for quasi-periodic oscillations, (f) Poincaré map for quasi-periodic oscillations.

Figure 5 shows the resonance curves for Case 2 considering softening behavior for the main structure and hardening behavior for the NLTVA. The nonlinear optimization is performed by fixing the amplitude of harmonic force F = 0.20 and varying the cubic stiffness of the absorber knl_2 to observe the resonance peaks as presented in Fig.5. As can be seen, for knl_2 equal to 1.00e-3 and 1.50e-3, the second resonance peak has higher amplitudes, while for knl_2 equal to 1.75e-3 and 2.00e-3, the first resonance peak shows higher amplitudes, then the optimal parameter was obtained for knl_2 equal to 1.625e-4.

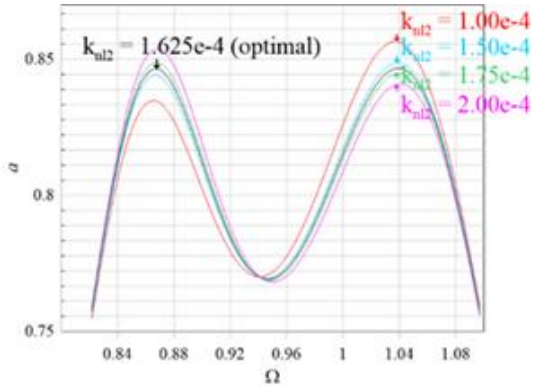

Figure 5. Nonlinear optimization for Case 2.

Figure 6 (a) shows the basin of attraction obtained for F = 0.20 N and Ω = 0.85. As can be observed, the basin of attraction has two attractors. Blue color attractor corresponds to stable 1T periodic oscillation and red color represents escape points (no convergence). In order to verify this behavior Fig. 6(b) shows the time response of a point with initial conditions in red color, as can be seen, there is no convergence and displacements grow continuously. Now, Fig. 6(c) and (d) show the time response and phase space of a point with initial conditions on the blue color attractor and, as observed, it displays stable 1T periodic oscillations. Finally, Fig. 6(e) shows the resonance curves for increasing values of amplitude of external load. As can be seen, for higher values of amplitude, the peaks of resonance curves are not equal which means the great sensitivity of the system to load amplitudes.

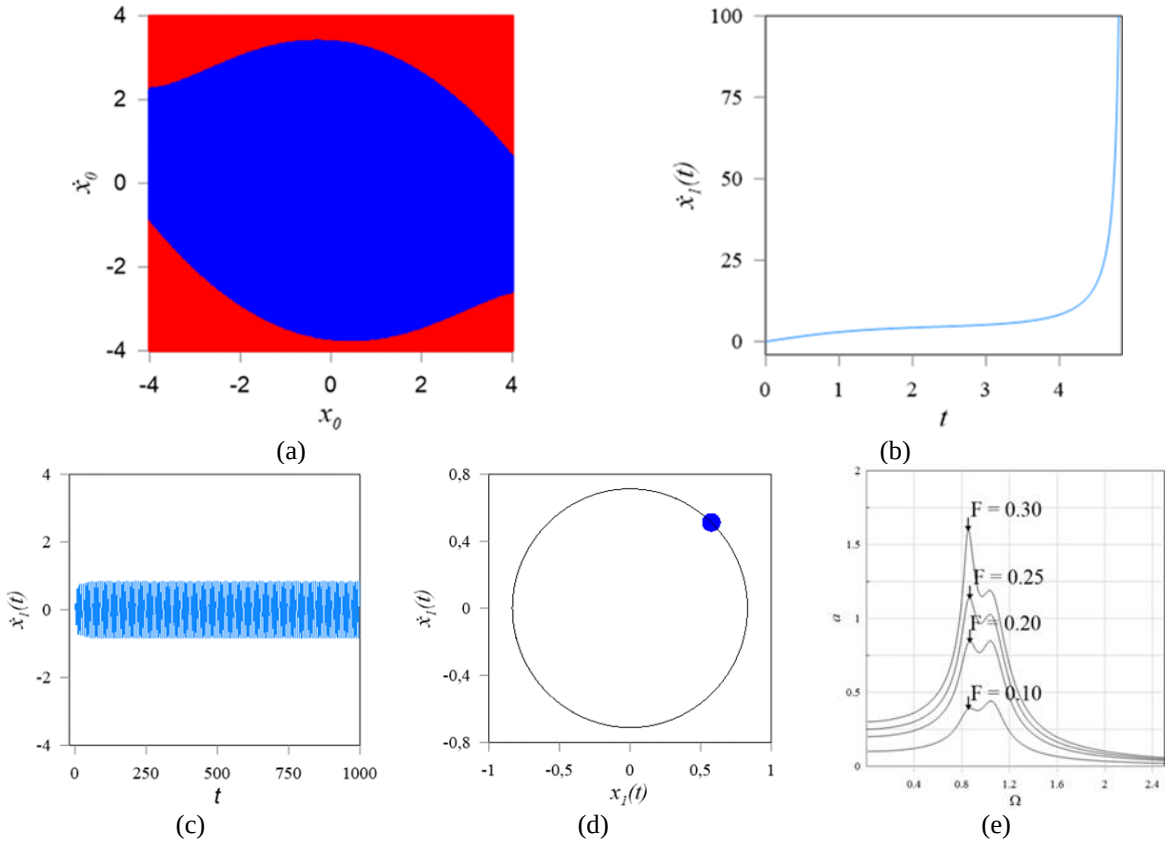

Figure 6. (a) Basin of attraction of the system studied in Case 2, for Ω = 0.85. (b) Time response for a point in the red zone. (c) Time response for a point in blue attractor. (d) Phase plane and Poincaré sections for a point in blue attractor. (e) Deoptimization of the system for different force amplitudes.

Now for Case 3, where both the main structure and the NLTVA display softening behavior. The nonlinear optimization of the system was attempted by fixing the harmonic force amplitude F = 0.20 and varying the cubic stiffness of the absorber knl_2 as depicted in Fig. 7(a). For negative knl_2 values as -1.0e-3 and -1.0e-4, the second resonance peak always displays higher amplitudes and equal peaks were not obtained for softening NLTVA. The optimal parameter was obtained for knl_2 = 1.625e-4, which is exactly the result obtained for Case 2.

Finally, for the Case 4, where the main structure depicts hardening behavior and the NLTVA depicts softening behavior, the nonlinear optimization was also attempted by fixing the harmonic force amplitude F = 0.05 and varying the cubic stiffness of the absorber knl_2 as seen in Fig. 7(b). As observed previously in Case 3, for Case 4 equal peaks couldn't be obtained for softening NLTVA and the optimal parameter was obtained for knl_2 = 4.0e-3, which is exactly the result obtained for Case 1.

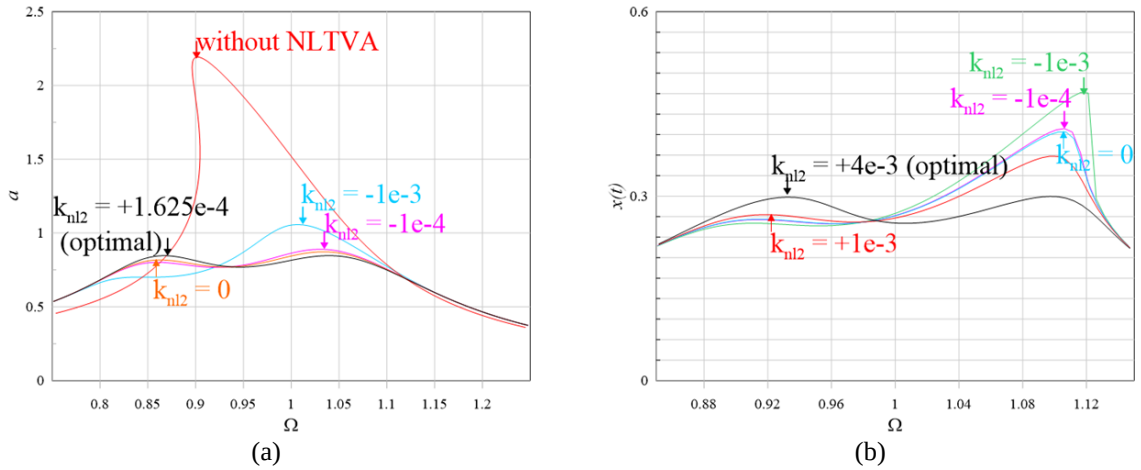

Figure 7. Non-linear optimization attempt for systems with softening NLTVAs. (a) Resonance curves for Case 3. (b) Resonance curves for Case 4.

Finally, the performance of the system is evaluated, for Cases 1 and 2, where the optimization was successfully obtained. Figure 8 shows a comparison between uncontrolled Duffing oscillator (red color) and controlled Duffing oscillator (blue color) with optimized NLTVAs.

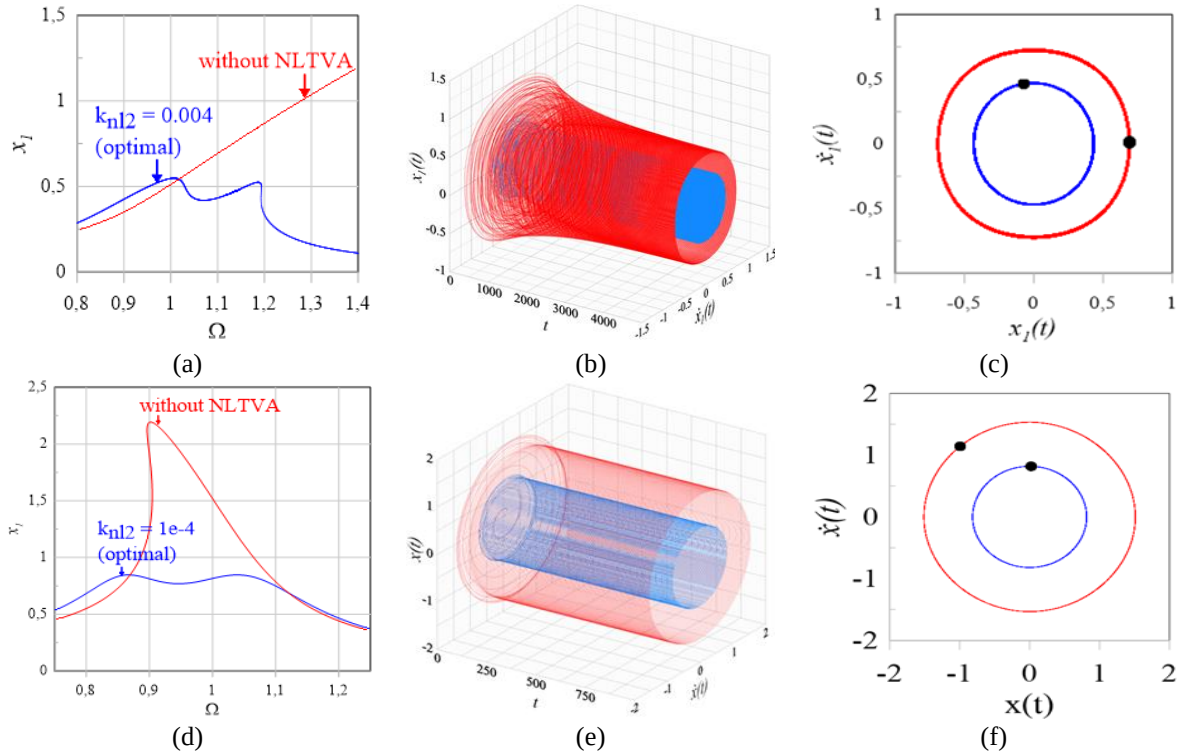

Figure 8. Comparison for the controlled (red) and uncontrolled (blue) Duffing oscillators. (a) Resonance curves for Case 1. (b) 3D plot representing displacements and velocities over time for Case 1. (c) Phase plane and Poincaré sections for Case 1. (d) Resonance curves for Case 2. (e) 3D plot representing displacements and velocities over time for Case 2. (f) Phase plane and Poincaré sections for Case 2.

Figure 8(a) displays the resonance curves comparing the controlled and uncontrolled system for Case 1 obtained for a value of harmonic force amplitude $F = 0.098$. As can be observed the NLTVA is effective only in a specific frequency range. For harmonic force frequencies Ω between 1.02 and 1.40, the NLTVA can highly

reduce the amplitude of displacements, in comparison with the uncontrolled system, while for Ω between 0.80 and 1.02, the displacements of the system with an attached NLTVA are slightly higher. The tridimensional plot in Fig. 8(b), where the displacements and velocities are depicted as a function of time, and the phase planes and Poincaré sections in Fig. 8(c) are obtained for $F = 0.098$ and $\Omega = 1.10$, where can be seen that the attachment of the NLTVA reduced the displacements amplitudes from values near 0.70 m to values near 0.50 m.

The same scenario was observed in the resonance curves presented in Fig. 8(d) for Case 2 and $F = 0.20$, where can be observed that the NLTVA was effective for values of harmonic force frequency Ω between 0.87 and 1.12, a smaller frequency range in comparison with the hardening main system depicted in Case 1. The time response of displacements and velocities in Fig. 8(e) and the phase planes and Poincaré sections in Fig. 8(f) were obtained for $F = 0.20$ and $\Omega = 1.00$, where the uncontrolled system has approximately 50% higher amplitudes for both displacements and velocities. For frequencies outside the effective frequency range, the attachment of the NLTVA slightly increases the displacement response of the structure.

4 Concluding remarks

This paper intended to analyze the performance of nonlinear systems composed by a damped Duffing oscillator with a nonlinear tuned vibration absorber (NLTVA) attached. The results show that the non-linear optimization was possible for hardening NLTVAs attached to both softening or hardening Duffing oscillators. For softening NLTVAs, the system wasn't optimal for any negative value of cubic stiffness k_{nl2}, always presenting higher resonance peaks than the optimized hardening NLTVA.

For both hardening and softening Duffing oscillators, the optimized NLTVA reduced significantly the steady-state vibrations for a specific range of harmonic force frequencies, as can be seen in Fig. 8 (a) and (d). The NLTVA presented a narrower frequency range of effectiveness when attached to a softening system rather than a hardening main system. For frequencies outside the effective range, the attachment of the NLTVA can increase the velocities and displacements amplitudes, so it is very important to observe this for engineering design applications.

For a softening Duffing oscillator, the system won't converge for initial conditions in the red attractor presented in the basin of attraction (Fig. 6 (a)). As the displacements increase hugely in a small period of time, this attractor represents an unsafe range of initial conditions, which needs to be avoided in a real engineering designing problem. Also, for a softening Duffing oscillator, the system showed a deoptimization for different amplitudes of harmonic forces F applied (Fig. 6(e)). The hardening Duffing oscillator is more robust, as the system still presents equal resonance peaks in a range of F between 0.005 and 0.11 N, as shown in Detroux *et al.* [6].

Authorship statement. The authors hereby confirm that they are the sole liable persons responsible for the authorship of this work, and that all material that has been herein included as part of the present paper is either the property (and authorship) of the authors or has the permission of the owners to be included here.

References

[1 H. Frahm. Device for Damping Vibrations of Bodies, US No. Patent 989958,1909.
[2] J. Ormondroyd; J.P. Den Hartog. The theory of the dynamic vibration absorber, Trans. ASME 50 (1928) 9–22.
[3] J. P. Den Hartog, Mechanical vibrations, New York: Dover Publications, 1985.
[4] Habib et al. 2015. Nonlinear generalization of Den Hartog′s equal-peak method, Mechanical Systems and Signal Processing, v. 52–53, p. 17–28, 2015.
[5] G. Habib; G. Kerschen. A principle of similarity for nonlinear vibration absorbers, Physica D: Nonlinear Phenomena, v . 332, p. 1–8, 2016.
[6] T. Detroux *et al*. Performance, robustness and sensitivity analysis of the nonlinear tuned vibration absorber, Mechanical Systems and Signal Processing, v. 60–61, p. 799–809, 2015.
[7] H.J. Korsch; J. Jodl, T. Hartmann. Chaos: a program collection for the PC., New York; London: Springer, 2008.
[8] T. Asami; O. Nishihara. Closed-Form Exact Solution to H∞ Optimization of Dynamic Vibration Absorbers (Application to Different Transfer Functions and Damping Systems), Journal of Vibration and Acoustics, v. 125, n. 3, p. 398–405, 2003.
[9] J. Connor; S. Laflamme, Structural Motion Engineering, 1st ed. 2014. Cham: Springer International Publishing: Imprint: Springer, 2014.
[10] Z. J. G. N. del Prado. Acoplamento e interação modal na instabilidade dinâmica de cascas cilíndricas. Tese (Doutorado em Engenharia Civil) – Departamento de Engenharia Civil, Pontifícia Universidade Católica do Rio de Janeiro, Rio de Janeiro, 2001.